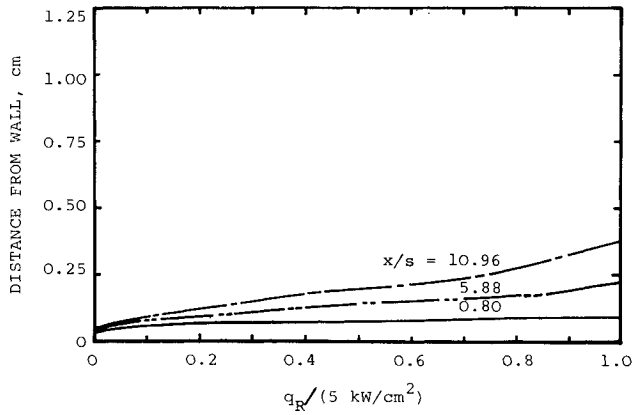

Fig. 4 Laser radiation profile in the boundary layer as a function of position along the flat plate.

ature occurs in the mixing layer between the air and the SF_6. The magnitude of the maximum temperature increases in the streamwise direction across the laser beam because the gas has absorbed more laser energy. At the far side of the laser beam, the temperature becomes so high that the SF_6 absorption coefficient is zero in part of the mixing layer (saturation). Consequently, radiation is absorbed above and below the high-temperature layer. This causes the adjacent gas to become hotter and the thickness of the high temperature layer to increase. The absorption of laser radiation and its subsequent heating increase the thermal boundary-layer thickness. SF_6 is dispersed farther into the airflow as the SF_6 is heated.

Figure 3 shows velocity profiles for $q_R(\delta) = 0$ and 5 kW/cm^2. At $x/s = 0.80$ for $q_R(\delta) = 0$, the velocity profile has a steplike jump in the mixing layer between the SF_6 and air, and the wake from the slot lip is evident. The velocities rapidly diffuse into a continuous profile downstream. Also, the boundary-layer thickness does not change very much with streamwise position for $q_R(\delta) = 0$.

When $q_R(\delta) = 5$ kW/cm^2, the boundary layer becomes thicker and the velocity profiles become smoother. The laser does not influence the velocity profile very much at $x/s = 0.80$. Further downstream, the absorption of laser energy reduces the air-side mixing layer velocity, because the slower moving SF_6 diffuses rapidly into the air since its temperature is higher. These effects reduce the velocity and increase the boundary-layer thickness.

The absorption coefficient of SF_6 increases as the partial pressure of SF_6 increases. Absorption of laser energy increases not only the temperature but also the partial pressure of SF_6 throughout the mixing layer relative to its value for $q_R(\delta) = 0$. Therefore, the temperature in the mixing layer is high compared to the temperature in the gas above and below it. The coupled increase of temperature and pressure causes the optical thickness of the boundary layer to increase when laser energy is absorbed.

Figure 4 shows the nondimensional laser flux $q_R/q_R(\delta)$ where $q_R(\delta) = 5$ kW/cm^2 as a function of distance across the boundary layer at three streamwise positions. Laser radiation does not reach the wall at any of the streamwise positions. The rapid diffusion of SF_6 into air is responsible for the reduction of the laser intensity further from the wall for increasing streamwise positions. At $x/s = 0.80$, the radiation penetrates much deeper into the boundary layer before it begins to be absorbed compared with $x/s = 10.96$.

Conclusions

Injection of SF_6 into the boundary layer is an effective way to absorb CO_2 laser radiation and to protect aerodynamic surfaces from CO_2 laser beams. The strong temperature dependence of the SF_6 absorption coefficient makes the boundary layer become transparent to the CO_2 laser radiation when the SF_6 temperature becomes greater than about 570°K. The absorbed energy couples strongly into the velocity, enthalpy, temperature, and composition profiles across the boundary layer. The energy absorption increases the diffusion rate of the SF_6 in the boundary layer.

References

[1]Hixson, B. A., Beckwith, I. E., and Bushnell, D. M., "Computer Program for Compressible Laminar or Turbulent Nonsimilar Boundary Layers," NASA TM X2140, April 1971.

[2]Beckwith, I. E. and Bushnell, D. M., "Calculation by a Finite-Difference Method of Supersonic Turbulent Boundary Layers with Tangential Slot Injection," NASA TN D-6221, April 1971.

[3]Cary, A. M., Bushnell, D. M., and Hefner, J. N., "Calculation of Turbulent Boundary Layers with Tangential Slot Injection," American Society of Mechanical Engineers Paper 77-WA/HT-27, Nov. 1977.

[4]Vincenti, W. G. and Kruger, C. H., *Introduction to Physical Gas Dynamics*, Wiley, New York, 1965, Chap. 12.

[5]Anderson, J. D., "A Numerical Analysis of CO_2 Laser Radiation Absorption in SF_6-Air Laminar Boundary Layers," Naval Ordnance Laboratory, Silver Spring, MD, NOLTR 73-143, July 1973.

[6]Anderson, J. D., "Computations of CO_2 Laser Radiation Absorption in SF_6-Air Boundary Layers," *AIAA Journal*, Vol. 12, Nov, 1974, pp. 1527–1533.

[7]Wagner, J. L. and Anderson, J. D., "Laser Radiation-Gasdynamic Coupling in the SF_6-Air Laminar Boundary Layer," *AIAA Journal*, Vol. 18, March 1980, pp. 333–334.

Melting of a Semitransparent Polymer Under Cyclic Constant Axial Stress

I. S. Habib*
University of Michigan—Dearborn, Dearborn, Michigan

Nomenclature

A_r = a constant related to the effect of temperature on viscosity
c = specific heat capacity
k = thermal conductivity of the solid
L = slab half-thickness
N_r = radiative conductive number = $(n^2\sigma T_1^3 L)/k$
N_s = inverse of Stefan number = $\lambda/T_1 c$
n = material index of refraction
q_r = radiative heat flux; $q_r^* = q_r/(n^2\sigma T_1^4)$
s = thickness of the solid phase; $s^* = s/L$
T = temperature; T_1 = cold boundary temperature; T_m = melt temperature
t = time; t also = dummy integration variable; $t^* = t\alpha/L^2$
x = distance from cold boundary
α = thermal diffusivity
β = heat generation parameter = $A_r \gamma L^2/k$; β_c = critical value of β
γ = heat generation per unit volume
δ = $A_r T_1$
κ = absorption coefficient
λ = latent heat of melting

Presented as Paper 87-1492 at the AIAA 22nd Thermophysics Conference, Honolulu, HI, June 8–10, 1987; received June 22, 1987; revision received March 21, 1988.

*Professor of Mechanical Engineering.

ξ = dimensionless distance from cold boundary = x/L
ρ = density of medium
σ = Stefan–Boltzmann constant
τ = optical depth = κL
ψ = dimensionless temperature = T/T_1; $\psi_m = T_m/T_1$

Introduction

In a previous study,[1,2] the thermal behavior of a semitransparent polymer subjected to a steady, cyclic axial stress was investigated accounting for the conductive and the radiative transfer processes. It was concluded that critical limits exist for the nonlinear heat generation induced by such loading. Beyond such limits, no thermal steady-state behavior is attained and the rate of heat generation within the solid exceeds the rate of heat transfer to the surrounding, thus creating an instability leading to what has been considered as a regime of solid disintegration. Similarity exists between this unstable condition and the thermal burst observed in the fluid flow with nonlinear viscous heat generation and the thermal explosion theory recognized in the exothermic chemical reactions.[3–9] A recent study on radiative ignition in a planar medium[10] showed a behavior similar to conductive ignition where both modes of ignition exhibit a discontinuity of the solution caused by the multisolution behavior, and a critical parameter is also identified in this case for stable solutions. Because the heat generation in a polymeric sample is exponentially dependent on the local temperature, the sample centerline becomes the starting position for sample failure. A distinct difference, however, exists between a polymeric solid sample and similar problems in fluid flow and chemical kinetics. In a physically realistic case of a solid polymer, an increase in cyclic frequency (and hence heat generation) is accompanied by a nonlinear increase in the centerline temperature up to the sample melting point. By maintaining the applied stress, a melting front is then created that propagates from the centerline towards the boundary.

The objective of this Note is to predict the position and speed of the melting front created in a polymeric sample by a cyclic loading with a constant stress amplitude. Planar geometry is considered, accounting for the coupled conductive and radiative heat-transfer processes. The time-dependent energy equation with nonlinear heat generation is solved using the integral technique. This approach proved to be very successful in analyzing phase-change problems with radiative transfer.[11,12]

Analysis

Figure 1 represents the model chosen for analysis. It is the one-dimensional melting of a semitransparent polymeric material subjected to a cyclic stress with constant stress amplitude. The resulting nonlinear heat generation is considered to be conducted and radiated toward the cooler boundary through the solid phase. A unique melt temperature T_m is assumed to exist and the liquid phase is maintained at that temperature. The melt line is treated as a plane surface with an emissivity equal to 1, while the cooler boundary is maintained at a constant temperature T_1 also with an emissivity equal to 1. The effect of surface emissivities in a phase-change planar problem has been treated before[12] and the effect of emissivities was to modify slightly the front speed and the temperature distribution in the solid. Hence, black boundaries are considered in the present study. The optical and thermophysical properties of the solid are taken as constant. Under such constraints the energy equation for the problem can be written in the following form:[1,2]

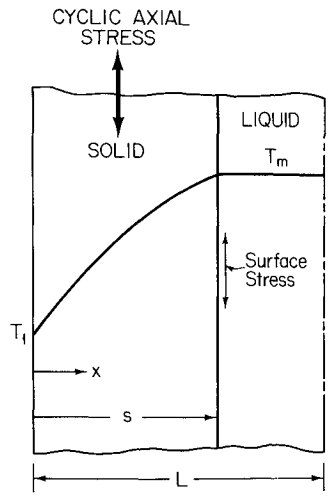

Fig. 1 The model chosen for the study.

$$\frac{1}{\alpha}\frac{\partial T}{\partial t} = \frac{\partial^2 T}{\partial x^2} - \frac{1}{k}\frac{\partial q_r}{\partial x} + \frac{\gamma}{k} e^{A_r(T-T_1)} \tag{1}$$

subject to the conditions

$$k\frac{\partial T}{\partial x} - q_r - \rho\lambda\frac{\mathrm{d}s}{\mathrm{d}t} = \gamma L e^{A_r(T_m - T_1)}, \qquad \text{at} \quad x = s \tag{2}$$

$$T(0,t) = T_1 \tag{3}$$

where the right-hand side of Eq. (2) represents a heat flux resulting from the surface axial stress at the solid-liquid interface. It is important to note here that the rate of heat generation in the solid phase varies from γ at $x = 0$, where $T = T_1$, to $\gamma e^{A_r(T_m - T_1)}$ at $x = s$, where $T = T_m$. The parameter γ is proportional to the square of the maximum shear stress amplitude and is maintained constant, and hence, the condition at $x = s$ must exhibit the same constant source of energy release for any position of the melt line. This source of surface-energy release is the only factor that drives the melt front. This is so because there is no position anywhere in the medium that can have a temperature higher than that of the interface in order to transfer energy to the interface and sustain the melting process. Although it is obvious that another boundary condition is given by

$$T(s,t) = T_m \tag{4}$$

this boundary condition is not appropriate for the present integral technique.[11] An alternate boundary condition is generated by differentiating Eq. (4) with respect to time and using Eq. (1) which results in the following expression as a condition at $x = s$.

$$\left[\frac{\partial T}{\partial x}\right]^2 = \frac{q_r}{k}\frac{\partial T}{\partial x} + \frac{\gamma L e^{A_r(T_m - T_1)}}{k}\frac{\partial T}{\partial x} - \frac{\lambda}{c}\frac{\partial^2 T}{\partial x^2} + \frac{\lambda}{ck}\frac{\partial q_r}{\partial x} - \frac{\lambda\gamma}{ck} e^{A_r(T_m - T_1)}, \qquad \text{at} \quad x = s \tag{5}$$

Casting Eq. (1) in dimensionless variables and integrating it between $\xi = 0$ and $\xi = s^*$, we obtain

$$(N_s + \psi_m)\frac{\mathrm{d}s^*}{\mathrm{d}t^*} = \frac{\mathrm{d}}{\mathrm{d}t^*}\int_0^{s^*} \psi(\xi)\,\mathrm{d}\xi + \left[\frac{\partial\psi}{\partial\xi}\right]_0 - [N_r q_r^*]_0 - \frac{\beta}{\delta} e^{\delta(\psi_m - 1)} - \frac{\beta}{\delta}\int_0^{s^*} e^{\delta(\psi - 1)}\,\mathrm{d}\xi \tag{6}$$

If we represent the temperature profile in the solid phase by a second-degree polynomial of the form

$$\psi_m - \psi = a(\xi - s^*) + b(\xi - s^*)^2 \tag{7}$$

then a and b are determined using Eqs. (3) and (5). When Eq. (7) is used in Eq. (6) and the integration is performed, the

following expression for the position of the dimensionless melt line s^* as a function of dimensionless time t^* is obtained.

$$\int_1^{s^*} \frac{\left[N_s - as^* - \left(\frac{s^*}{2}\right)^2 \frac{da}{ds^*} + s^{*3}\frac{db}{ds^*} + bs^{*2}\right] ds^*}{2bs^* - a - (N_r q_r^*)_0 - \frac{\beta}{\delta} e^{\delta(\psi_m - 1)} - \frac{\beta}{\delta}\int_0^{s^*} e^{\delta(\psi - 1)}\, ds^*} = t^* \tag{8}$$

Results and Conclusions

Equation (8) is solved by the method of successive substitution to yield s^* vs t^*. Two values of N_s (inverse of Stefan number), one value for the radiation-conduction number N_r, and values for the heat-generation parameter β ranging from 1 to 10 are used. It is important to indicate that melting can proceed only for β greater than the critical value for pure conduction, namely, 0.88.[1,2,9] For β below this value, a thermal steady state can exist in which the heat generation is balanced by the heat transfer to the ambient by both conduction and radiation. For β greater than 0.88, no steady state exists for pure conduction and the centerline temperature of the solid increases indefinitely with the applied cyclic stress. It is this regime that leads to sample melting. As concluded in previous work,[1,2] the critical value for β increases when radiation is included in the analysis.

Figure 2 shows the time it takes to melt 50% of a polymeric slab as a function of the heat-generation parameter β. The results are for optical depths of 0, 1, and 5 plus the pure conduction case. As β decreases from a high value, the time t^* increases and the curves appear to approach in an asymptotic way to the line representing the critical value for β. Below that critical value of β_c as mentioned earlier, no melting would take place. The effect of the optical depth is most significant at low values of β. For $\beta > 2$, and for the conditions of the present problem, the time it takes to melt 50% of the solid becomes practically independent of the optical properties and the radiative transfer. In this range, the results can be described adequately by the pure conduction solution.

Table 1 shows representative results for the time and position of the solid-liquid interface in a polymeric slab subjected to one level of heat generation, $\beta = 2$, and for two values of N_s. The case of a nonradiating opaque slab ($N_r = 0$) and the cases for radiating slabs with a radiation-conduction number $N_r = 0.135$ are presented. It is shown that when $\beta = 2$, the slab with an absorption coefficient $\kappa = 0$ exhibits, in general, a slower rate of melting than the nonradiating (opaque) slab and also slower than the other radiating slabs. During the early stages of melting, however, the case with an absorption coefficient $\kappa = 3.28\ \text{m}^{-1}$ (optical depth = 1) exhibits a slower rate than that with $\kappa = 0$. This behavior appears to be somehow unusual when compared with the cases with no heat generation.[11,12] When consideration is given to the temperature distribution presented in Fig. 3, it can be seen that the case with $\kappa = 0$ shows a higher temperature than the pure-conduction case ($N_r = 0$). Increasing the absorption coefficient in the medium ultimately drives the temperature below the conduction case. In the absence of heat generation, such a trend in the temperature distribution coupled to the interface-movement speed resulted in the conclusion that the case for $\kappa = 0$ must yield an upper bound on time for melting while the opaque case provides a lower bound. With the heat generation being exponentially dependent on temperature, a higher temperature in the medium augments the heat generation exponentially and brings the solid faster to the melting level. On the other hand, with $\kappa = 0$, the medium is transparent to radiation and radiative energy is transmitted directly to the cooler boundary, thus decreasing the magnitude of the flux available at the interface for melting. Accordingly, $\kappa = 0$ may no longer represent an upper bound for melting time.

Table 1 Position and time of the solid-liquid interface for $\beta = 2$; $T_1 = 300$°K; $T_m = 417$°K; $n = 1.5$; $\delta = 5.86$; $L = 0.305$ m; $\lambda = 23.3$ kJ/kg; $k = 7.78$ W/m°C; $c = 837$ J/kg°C; $\rho = 2403$ kg/m³

	t^*				
	$N_r = 0.135$				
		Absorption coefficient κ, m^{-1}			
s^*	$N_r = 0$	16.4	3.28	1.64	0
		$N_s = 0.370$			
0.90	0.014	0.016	0.016	0.015	0.014
0.80	0.029	0.033	0.032	0.032	0.030
0.70	0.044	0.050	0.050	0.049	0.047
0.60	0.061	0.068	0.068	0.067	0.065
0.50	0.079	0.087	0.088	0.087	0.085
0.40	0.099	0.107	0.111	0.111	0.110
0.30	0.125	0.132	0.141	0.142	0.143
0.20	0.179	0.183	0.225	0.238	0.257
		$N_s = 0.741$			
0.90	0.023	0.024	0.025	0.025	0.024
0.80	0.047	0.050	0.052	0.052	0.051
0.70	0.072	0.075	0.080	0.080	0.079
0.60	0.099	0.102	0.109	0.110	0.109
0.50	0.129	0.131	0.141	0.143	0.143
0.40	0.163	0.162	0.178	0.180	0.183
0.30	0.204	0.200	0.224	0.229	0.234
0.20	0.278	0.265	0.321	0.337	0.351

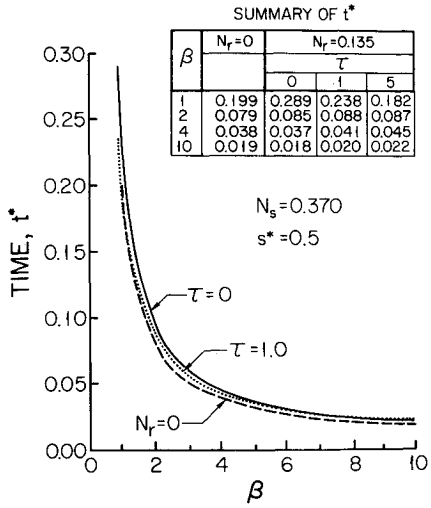

Fig. 2 The effect of the heat-generation parameter on melting time.

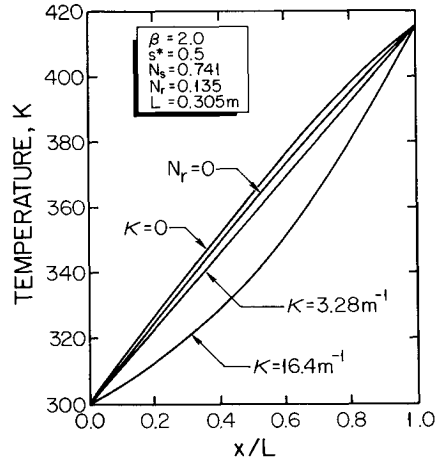

Fig. 3 The effect of the absorption coefficient on the temperature distribution.

This behavior was observed also for higher values of β. Furthermore, when consideration is given to the fact that the radiative-conductive interaction is most significant for an optical depth of order 1, such a behavior, then, can be further justified.

References

[1]Habib, I. S., "Radiative and Convective Effects on the Vibrational Heating of Semitransparent Polymers," *Journal of Spacecrafts and Rockets*, Vol. 23, Jan. 1986, pp. 124–126.

[2]Habib, I. S., "Radiation Effects on Vibrational Heating of Polymers," *Journal of Spacecrafts and Rockets*, Vol. 21, May 1984, pp. 496–501.

[3]Meinkoh, D., "Heat Explosion Theory and Vibrational Heating of Polymers," *International Journal of Heat and Mass Transfer*, Vol. 24, April 1981, pp. 645–648.

[4]Stolin, A. M., Bostandzhiyan, S. A., and Plotnikova, N. V., "Conditions for Occurrence of Hydrodynamic Thermal Explosion in Flows of Power-Law Fluids," *Heat Transfer—Soviet Research*, Vol. 10, 1978, pp. 86–93.

[5]Ayeni, R. O., "On the Thermal Runaway of Variable Viscosity Flows Between Concentric Cylinders," *Zeitschrift für Zangewandte Mathematik und Mechanik*, Vol. 23, 1982, pp. 408–413.

[6]Buevich, Y. A. and Zaslvaskii, M. I., "Hydrodynamic Thermal Burst in Radial Bearing," *Journal of Engineering Physics*, Vol. 42, 1982, pp. 566–571.

[7]Gray, P. and Lee, P. R., "Thermal Explosion Theory," *Oxidation and Combustion Reviews*, Vol. 2, 1967, pp. 1–183.

[8]Steggerda, J. J., "Thermal Stability: An Extension of Frank-Kamenetskii's Theory," *Journal of Chemical Physics*, Vol. 43, 1965, pp. 4446–4448.

[9]Frank-Kamenetskii, D. A., *Diffusion and Heat Transfer in Chemical Kinetics*, Plenum Press, New York, 1969, pp. 236–265.

[10]Crosbie, A. L. and Pattabongse, M., "Radiative Ignition in a Planar Medium," Thermal Radiative Transfer Group, Dept. of Mechanical Engineering, Univ. of Missouri—Rolla (submitted for publication).

[11]Habib, I. S., "Solidification of a Semitransparent Cylindrical Medium by Conduction and Radiation," *Journal of Heat Transfer*, Transactions of the American Society of Mechanical Engineers, Vol. 95, Ser. C, No. 1, 1973, pp. 37–41.

[12]Habib, I. S., "Solidification of a Semitransparent Material by Conduction and Radiation," *International Journal of Heat and Mass Transfer*, Vol. 14, Dec. 1971, pp. 2161–2164.

Solidification Heat Transfer on a Moving Continuous Cylinder

F. B. Cheung* and S. W. Cha†
Pennsylvania State University, University Park, Pennsylvania

Introduction

WHEN a continuous cylinder is caused to travel axially through a large bath of warm liquid, a boundary-layer type of flow will be induced in the liquid phase adjacent to the solid boundary.[1] If the cylinder is precooled below the freezing point of the liquid before entering the bath, a solidified layer or freeze coat will form on the surface of the moving object. This solidification process, known as freeze-coating, is an important material manufacturing process with applications in the electrical and chemical industries for casting insulating coatings on metal wires or electricity cables.

Seeniraj and Bose[2] studied the freeze-coating problem by assuming the moving object to be isothermal and the liquid to be saturated at its freezing point. Cheung[3,4] investigated the problem of freeze-coating of a superheated liquid on a continuous moving plate by including the effects of temperature variation within the plate and heat convection from the warm liquid. For a moving cylinder, two asymptotic solutions were presented by Cheung and Cha.[5,6] The first solution was obtained under the condition of negligible interaction between the freeze coat and the liquid flowfield; the second solution was obtained under the condition of negligible radial variation of the cylinder temperature.

In this study, a general solution is sought by the finite-difference method for freeze-coating of a superheated liquid on a nonisothermal axially moving cylinder, taking full account of mutual interaction between the freeze coat and the liquid flowfield, as well as variation of the cylinder temperature in the radial and axial directions.

Mathematical Model

To formulate the problem mathematically, the frame of axes are chosen to be stationary with respect to the liquid bath (Fig. 1). The freeze-coating process is considered to take place at a steady state and at a constant freezing temperature of the liquid. Under these conditions, the equations governing the liquid velocity, liquid temperature, freeze-coat temperature, cylinder temperature, and the axial variation of the freeze-coat thickness can be written as follows:

Boundary-Layer Flow Region, $r \geq \delta(x)$

$$r\frac{\partial u}{\partial x}+\frac{\partial (vr)}{\partial r}=0 \tag{1}$$

$$u\frac{\partial u}{\partial x}+v\frac{\partial u}{\partial r}=\frac{\nu}{r}\frac{\partial}{\partial r}\left(r\frac{\partial u}{\partial r}\right) \tag{2}$$

$$u\frac{\partial T}{\partial x}+v\frac{\partial T}{\partial r}=\frac{\alpha}{r}\frac{\partial}{\partial r}\left(r\frac{\partial T}{\partial r}\right) \tag{3}$$

$$x=0: \quad u=0, \qquad T=T_\infty > T_f \tag{4a}$$

$$r=\delta(x): \quad u=U, \qquad v=0, \quad T=T_f \tag{4b}$$

$$r\to\infty: \quad u=0, \qquad T=T_\infty \tag{4c}$$

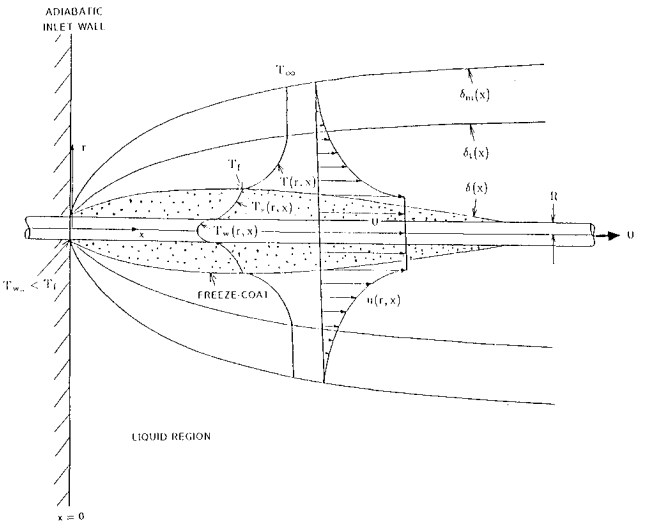

Fig. 1 Schematic of the freeze-coat on a nonisothermal axially moving continuous cylinder, indicating nomenclature.

Received May 9, 1988; presented as Paper 88-2642 at the AIAA Thermophysics, Plasmadynamics, and Laser Conference, San Antonio, TX, June 27–29, 1988; revision received Aug. 31, 1988.

*Associate Professor, Mechanical Engineering Department.

†Graduate Assistant, Mechanical Engineering Department; currently, Assistant Professor, Suwon University, South Korea.